

A Role of Cell Apoptosis in Lipopolysaccharide (LPS)-induced Nonlethal Liver Injury in D-galactosamine (D-GalN)-sensitized Rats

Liang-Ming Liu · Ji-Xiang Zhang · Jie Luo · Hong-Xing Guo · Huan Deng · Jian-Yong Chen · Sui-Lin Sun

Received: 10 March 2007 / Accepted: 20 August 2007 / Published online: 13 October 2007
© Springer Science+Business Media, LLC 2007

Abstract Lipopolysaccharide (LPS) is implicated in the pathology of acute liver injury and can induce lethal liver failure when simultaneously administered with D-galactosamine (D-GalN). At the present time, nonlethal liver failure, the liver injury of clinical implication, is incompletely understood following challenge by low-dose LPS/D-GalN. We report here our investigation of the effects of liver injury following a nonlethal dose LPS/D-GalN and the role of apoptosis in this disorder. Blood biochemistry indexes, including those of alanine aminotransferase (ALT), aspartate aminotransferase (AST) and total bilirubin (TBIL), had risen by 6 h post-LPS/D-GalN injection, reached a peak at 24 h and sustained high levels at 48 h. An abnormal liver appearance was found at 24 and 48 h post-injection. Histopathological changes of hepatic injuries accompanied by hepatocellular death, inflammatory infiltration and hemorrhage began to appear at 6 h and were markedly aggravated at 24 and 48 h. Cell apoptosis was significantly induced by the nonlethal dose LPS/D-GalN challenge, and the apoptotic indexes (AIs) in 24 h- and 48 h-treated rats were approximately 70%, as estimated by the terminal transferase dUTP nick end labeling (TUNEL) assay. The mRNA levels of the inflammatory cytokine IL-1 β rose markedly at 6 h and maintained high levels at 24 and 48 h; however, TNF- α

levels were normal in the liver tissues of 6-, 24- and 48-h-treated rats. mRNA expression of the damage gene nitric oxide synthase (NOS) was also induced early by the LPS/D-GalN challenge, reaching a peak at 6 h, then gradually decreasing in a stepwise manner; conversely, high expression levels of the apoptosis-inducing gene p53 mRNA were not found in the early post-injection period (6 h) but emerged in the crest-time of liver apoptosis (24 h) and were maintained at this level until the late stage (48 h). We also observed that in 24 h-treated rats, caspase-3, -8, -9 and -12 were markedly activated by LPS/D-GalN challenge. These results suggest that a challenge with low-dose LPS in conjunction with D-GalN can induce nonlethal but marked liver failure, the main morphological feature of which is hepatic apoptosis, which may be associated with a high expression of inducible (i)NOS (early post-injection period) and p53 genes (in the mid and late stages) and at least three apoptosis pathways participate in the pathogenesis.

Keywords Cell apoptosis · D-Galactosamine · Lipopolysaccharide · Nonlethal liver injury

Introduction

Lipopolysaccharide (LPS), the major structural component of the outer membrane of Gram-negative bacteria, plays a pivotal role in endotoxemia. In the past 20 years, there has been a steadily increasing incidence of endotoxemia, mostly because increasingly more patients are immunocompromised from HIV infection and immunosuppressive drugs and undergoing cancer therapy and invasive surgical procedures. Lipopolysaccharide enters the body mainly from the intestine. Under normal conditions, a small amount of LPS can periodically be taken up into the liver through the

L.-M. Liu · J.-X. Zhang (✉) · J. Luo · H.-X. Guo · H. Deng · J.-Y. Chen · S.-L. Sun
Department of Gastroenterology, Second Affiliated Hospital, Nanchang University, Nanchang, Jiangxi Province 330006, China
e-mail: jixiangz@tom.com

L.-M. Liu · J.-X. Zhang · J. Luo · H.-X. Guo · H. Deng · J.-Y. Chen · S.-L. Sun
Jiangxi Province Key Laboratory of Molecular Medicine, Nanchang, Jiangxi Province 330006, China

portal vein and then scavenged by Kupffer cells (KCs), the resident macrophages in the liver. In patients with severe trauma, burn, intestinal ischemia and liver diseases, LPS can spill over into the systemic circulation because of the increased permeability of the intestinal wall and/or the decreased phagocytic ability of liver KCs; this condition is called intestinal endotoxemia (IETM). As the liver functions as the first barrier to LPS entering into circulation and as a detoxication organ, it is deeply impacted by endotoxemia, especially IETM. In recent years, researchers have focused increasing attention on the damaging effects of LPS on the liver. The hepatotoxicity of LPS is mainly dependent on the production and release of potent inflammatory mediators, such as tumor necrosis factor alpha (TNF- α), interleukin 1 β (IL-1 β), IL-6, among others [1, 2]. These immunological mediators, especially TNF- α , can induce apoptotic liver injury and the infiltration of inflammatory cells. The latter, in turn, can further exacerbate liver injury, which continues the vicious circle of infiltration/liver injury.

A reasonable approach to gaining an insight into the pathophysiological processes involved in LPS-induced liver injury is to establish an appropriate animal model. However, to date, this has proven to be a difficult task since rodents are commonly resistant to LPS. High-dose LPS challenge can cause not only the loss of hepatic function but also multiple organ failure associated with severe sepsis – i.e. LPS-induced systemic toxicity [3, 4]. Galanos et al. [5] reported that the simultaneous administration of D-galactosamine (D-GalN) to experimental animals is able to greatly increase the sensitivity of these animals to the lethality of LPS. Although D-GalN does not stimulate the release of inflammatory mediators and alter liver function, by reversibly depleting hepatic stores of uridine triphosphate (UTP), it can increase LPS lethality by more than 2500-fold in experimental mice [5]. In contrast to the high-dose LPS-induced systemic disorder, the liver is a major target organ after challenge with low-dose LPS in conjunction with D-GalN [5, 6]. The lethal effects of LPS in mice sensitized with D-GalN are known to be due to the hepatotoxic effects of LPS-induced TNF- α [5, 7] and, therefore, LPS/D-GalN-induced hepatitis is a well-established model of LPS-induced liver injury or septic shock [5, 8–13]. However, the pathogenesis, morbid state and pathological process of LPS/D-GalN-induced acute liver damage in sublethal dose have remained elusive. An experimental animal challenged with a nonlethal amount of LPS/D-GalN may be of clinical importance as a number of inflammatory liver diseases in humans, including viral hepatitis, alcoholic liver disease, immune- or drug-induced liver injury and ischemia/reperfusion liver failure, have been shown to be dependent on TNF- α production [14–19]. Therefore, the rat model may provide a valuable approach

to study acute liver injury mediated by inflammatory cytokines.

The aim of this study was to examine the effects of hepatic injury of a nonlethal dose of LPS/D-GalN and the role of hepatocellular apoptosis in LPS/D-GalN-induced acute liver failure. We wished to provide a well-defined and reliable animal model to screen or investigate anti-hepatitis drugs for the future.

Material and methods

Animal procedures

Healthy male Wistar rats weighing 200 ± 10 g obtained from the Animal Scientific Department, Medical College of Nanchang University, Nanchang, China were used in this study. Animal protocols were approved by the Institutional Review Board according to the Animal Protection Act of China. *Escherichia coli* endotoxin (LPS) and D-GalN were purchased from Sigma Chemical Co (St. Louis, MO). Rats were injected intraperitoneally with 10 μ g LPS (50 μ g/kg) and 60 mg D-GalN (300 mg/kg) dissolved in 1 ml of sterile pyrogen-free 0.9% sodium chloride [5]. Control animals were intraperitoneally injected with an equal volume of 0.9% sodium chloride. Eight animals of each group at each time point were killed at 6, 24 and 48 h after injection, blood samples from portal vein were collected for measuring the activities of the liver enzymes alanine aminotransferase (ALT) and aspartate aminotransferase (AST) and levels of total bilirubin (TBIL) using an auto-assay meter of blood biochemistry and the livers were excised quickly and preserved in liquid nitrogen. The remaining liver tissues were fixed with 4% paraformaldehyde for hematoxylin and eosin (HE) staining or for the terminal transferase dUTP nick end labeling (TUNEL) assay. For electron microscopy, the livers were immersed in glutaraldehyde.

Histology examination

The liver tissues fixed in 4% paraformaldehyde were paraffin-embedded and cut into 6- μ m sections which were then stained with HE for analysis under the light microscope. The livers immersed in glutaraldehyde were carefully prepared for transmission electron microscopy.

TUNEL assay

The assessment of liver apoptosis was performed using DeadEnd Colorimetric TUNEL assays according to the

manufacturer's instructions (Promega, Madison, WI). Briefly, the paraffin was removed from paraffin-embedded liver sections using xylene and the liver sections fixed again in 4% formaldehyde. The sections were permeabilized with a solution of proteinase K, labeled with terminal transferase (TdT) reaction mix and then bound in streptavidin HRP solution. The sections were then stained by diaminobenzidine (DAB) with chromogen horseradish peroxidase and subsequently incubated with diaminobenzidine substrate to produce a dark-brown precipitate and then counterstained slightly with hematoxylin. The positive cells in the stained sections were identified and counted under a light microscope.

Reverse transcriptase-PCR

Total RNA was extracted from liver tissues with TRIzol reagent (Invitrogen, Carlsbad, CA) following the manufacturer's instructions. The amount and integrity of the RNA preparations were assessed by spectrophotometry and agarose gel electrophoresis. A 2-mg sample of total RNA was used as the template for synthesis of first-strand cDNA with a M-MLV RT kit (Promega). The PCR primers were designed using PRIMER PREMIER ver. 5.0 software (PremierBiosoft, Palo Alto, CA) from the reported sequences [GenBank accession nos. X66539 for TNF- α , NM031512 for IL-1 β , NM012611 for nitric oxide synthase (NOS), NM030989 for p53 and NM031144 for β -actin]. The following oligonucleotide primers were used: (1) TNF- α : sense, 5'-CTGGGCAGCGTTTATTCT-3'; antisense, 5'-TGCTTCTTCCCTGTTCC-3' (product length 249 bp); (2) IL-1 β : sense, 5'-CCTTCTTTTCCTTCATCTTTG-3'; antisense, 5'-ACCGCTTTTCCATCTTCTTCT-3' (product length 372 bp); (3) inducible (i)NOS: sense, 5'-ATCCGAAACGCTACACTT-3'; antisense, 5'-AATCCACA ACTCGCTCCA-3' (product length 301 bp); (4) p53: sense, 5'-TGGAGGATTCACAGTCCG-3'; antisense, 5'-GGTGGAAGCCATAGTTGC-3' (product length 324 bp); (5) β -actin: sense, 5'-ACACTGTGCCCATCTACGAGG-3'; antisense, 5'-AGGGGCCGGACTCGTCATACT-3' (product length 621 bp). The thermal cycling conditions of the PCR assays for TNF- α or IL-1 β and β -actin were: denaturation at 95°C for 5 min, followed by 38 cycles of denaturation at 95°C for 45 s, primer annealing at 55°C for 45 s and primer extension at 72°C for 1 min, with a final extension at 72°C for 6 min. The thermal cycling conditions of the PCR assays for iNOS and β -actin were: denaturation at 95°C for 4 min, followed by 35 cycles of denaturation at 94°C for 1 min, primer annealing at 51°C for 1 min and primer extension at 72°C for 1 min, with a final extension at 72°C for 3 min. The PCR assays for p53 and β -actin were performed using thermal cycling

conditions consisting of denaturation at 95°C for 5 min, followed by 37 cycles of denaturation at 95°C for 45 s, primer annealing at 53°C for 45 s and primer extension at 72°C for 1 min, with a final extension at 72°C for 6 min. The PCR products were run on a 1.5% agarose gel and subjected to densitometric scanning using the Epson 165 photo scanner (EPSON, Belgium), and the bands were quantified with NIH IMAGE ver. 1.62 software. The level of a particular cDNA was normalized to that of the β -actin product.

Caspase assays

Caspase-3, -8, -9 and -12 activities in liver tissue were measured using the Caspase Fluorometric Assay kit (Bio-Vision, Mountain View, CA) according to the manufacturer's instructions and a modified protocol. Briefly, liver tissues were homogenized in lysis buffer to generate tissue lysate. The homogenates were centrifuged at 15,000 rpm at 4°C for 10 min and the supernatants used for subsequent analyses. The protein concentration of the samples was determined by the Bradford method using bovine serum albumin as standard. A 20- to 200- μ g aliquot of each sample of extracted proteins was tested in duplicate experiments with 50 μ M final concentration of fluorescent substrates for caspase-3 [DEVD-AFC (7-amino-4-trifluoromethyl coumarin)], caspase-8 (IETD-AFC), caspase-9 (LEHD-AFC) or caspase-12 (ATAD-AFC) at 37°C for 1–2 h. The levels of AFC released by enzymatic reaction were measured on a spectrofluorometer (model F-4500 FL; Hitachi) using an excitation wavelength of 400 nm and an emission wavelength of 505 nm. Caspase activity was expressed in picomoles per minute per milligram of protein.

Statistics

Data for the experiments were expressed as means \pm SD. Single-factor analysis of variance (ANOVA) was performed for each group, and significance was assumed at $P \leq 0.05$. Differences among means were compared using the Student's t test.

Results

Abnormal blood biochemistry associated with the administration of LPS and D-GalN

Serum ALT, AST and TBIL levels provide indexes of hepatocyte integrity and bile metabolism. As such, any

increase in these indexes in the serum reflects hepatic dysfunction or liver damage. As shown in Table 1, serum ALT, AST and TBIL levels increased significantly at 6 h post-, reached the peak at 24 h and sustained high levels at 48 h although all the animals survived until being killed after administration of LPS and D-GalN. The ALT levels, however, were significantly lower in the 48-h-treated rats than those in the 24-h-treated rats ($P < 0.01$), which might reflect a significant but reversible hepatic injury.

Changes in the macroscopic appearance of the liver results from LPS/D-GalN injection

Normally shaped like a cone, the liver is a dark reddish-brown organ that has glossy tegument and soft texture. As shown in Fig. 1, the liver of the treated rats was swollen and pale with a tenacious texture and had sporadic, punctiform and lamellar hemorrhagic spots on its surface. This demonstrated that significant liver damage had been induced with a sublethal dose of LPS/D-GalN.

Histopathological changes in the livers after simultaneous administration of LPS and D-GalN

The liver sections of control rats showed an integrated structure of hepatic lobule, and there were no denatured or necrotic hepatocytes (Fig. 2A). Under the electron microscope, the control liver sections only rarely contained apoptotic cells. Figure 3A shows a control or normal hepatic cell with an ovate nucleus and profuse mitochondria

and endoplasmic reticulum system in the cytoplasm. The injection of LPS into D-GalN-sensitized rats induced marked hepatic injuries accompanied by hemorrhage and death of hepatic cells. The liver sections taken from 6 h-treated rats presented the features of piecemeal necrosis, inflammatory infiltration and congestion (Fig. 2) and dispersed apoptotic cells. Figure 3B shows a typical apoptotic cell in the liver tissues of 6 h-treated rats; typical ultrastructural features include chromatin aggregation and condensation, nuclear cavitations and condensing cytoplasm with swollen mitochondria. Characteristic features of cellular vacuolar degeneration, engorgement, focal necrosis, neutrophil infiltration and erythrocyte agglutination were observed in the liver sections of 24 h-treated rats (Fig. 2C), and bulks of apoptotic cells were found in liver tissues examined under the electron microscope. During this stage, marginalization and fragmentation of chromatin occurred, and the nuclei loosed their round or oval shape, budded and become fragmented – apoptotic bodies were formed (Fig. 3C). In the liver tissues of 48-h-treated rats, vacuolar degeneration appeared in a majority of liver cells, and structural disorder of the liver lobule and spot necrosis were detected Fig. 2D. Electron microscopy of the liver sections of 48-h-treated rats revealed multitudes of apoptotic cells. At this stage, karyopyknosis, chromatin marginalization, apoptotic bodies and swollen or fatted mitochondria were the characteristics of apoptotic liver cells (Fig. 3D). These results reveal that although a slight liver injury or cell apoptosis emerged as early as 6 h post-LPS/D-GalN injection, marked liver injury and massive numbers of late apoptotic cells and apoptotic bodies did not occur until 24 h post-injection.

Table 1 Serum alanine aminotransferase (ALT), aspartate aminotransferase (AST) and total bilirubin (TBIL) levels in rats following lipopolysaccharide-D-galactosamine (LPS/D-GalN) injection

Groups	Time post-LPS/D-GalN injection (h)	ALT (u/L)	AST (u/L)	TBIL ($\mu\text{mol/L}$)
Control rats		66.0 \pm 3.2 a	316.9 \pm 37.5 a	9.4 \pm 1.2 a
Treated rats	6h	398.6 \pm 83.0 b	634.1 \pm 112.2 b	15.8 \pm 6.7 b
	24	3178 \pm 635 b,c	4027 \pm 943 b,c	59.6 \pm 8.7 b,c
	48	1506 \pm 566 b,c,d	3961.4 \pm 820 b,c	58.8 \pm 10.1b,c

Letters following values indicate: b, $P < 0.01$ vs. control rats; c, $P < 0.01$ vs. 6 h-treated rats; d, $P < 0.01$ vs. 24 h-treated rats

Fig. 1 Macroscopic appearance of the rat liver. **A** Control, **B** 24 h-treated group, **C** 48 h-treated group

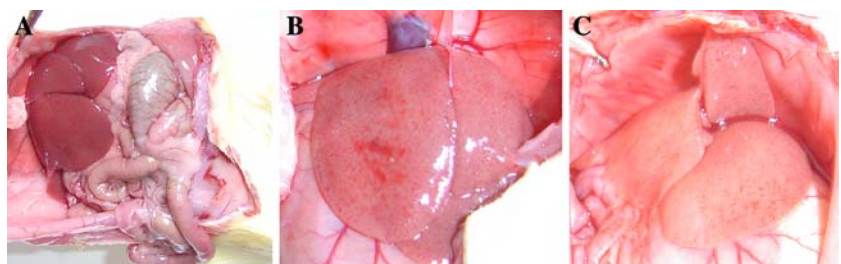


Fig. 2 Histology of liver sections from control and treated rats following lipopolysaccharide-D-galactosamine (LPS/D-GalN) administration. **A** Control, **B** 6-h-treated groups, **C** 24-h-treated groups, **D** 48-h-treated groups

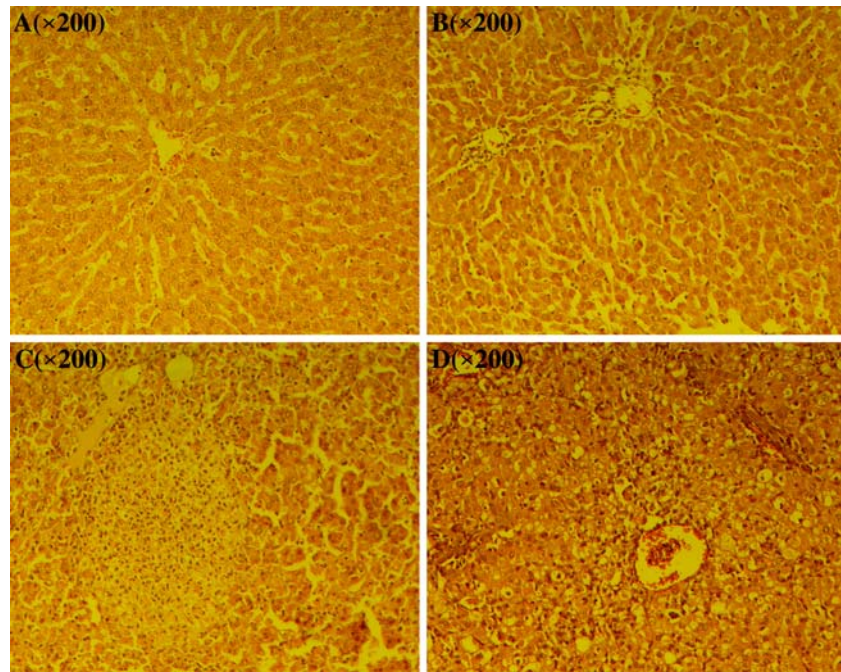
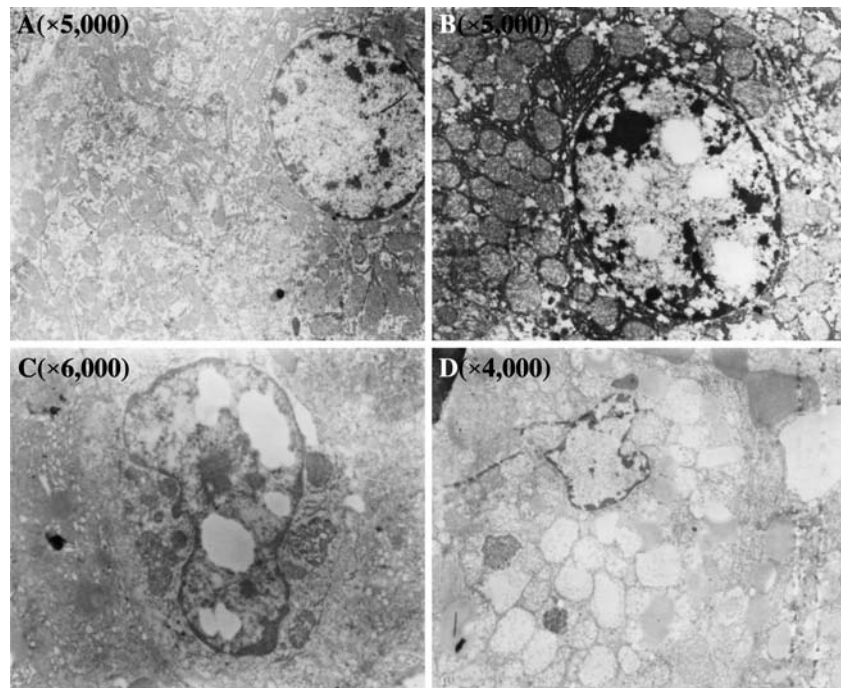


Fig. 3 Ultrastructural features of liver tissues from control and treated rats. **A** Control, **B** 6-h-treated group, **C** 24-h-treated group, **D** 48-h-treated group



Massive apoptosis of liver was induced by LPS/D-GalN challenge through TUNEL assay

The TUNEL assay is a sensitive method for appraising cell apoptosis. In this test, the percentage of apoptotic cells with positive nuclei is calculated in the most frequently identified areas; this percentage is then referred to as the apoptotic index (AI). We examined a minimum of 1000

cells per section in five randomly selected fields by light microscopy ($\times 400$). At least four sections were used for calculating the AI means of each group cells. The characteristic morphology of apoptotic cells was frequently observed under the light microscope, including cell shrinkage, nuclear chromatin condensation and the formation of cytoplasmic blebs and apoptotic bodies. The AIs in the control, 6-h-, 24-h- and 48-h-treated groups were

2.6 ± 1.1 , 7.3 ± 1.5 , 71.8 ± 10.3 and $68.2\% \pm 11.9\%$, respectively. As shown in Fig. 4, compared with the control, the AIs in the treated groups were significantly enhanced ($P < 0.01$); in addition, the AIs in the 6-h-treated group were significantly lower than those in the 24-h- and 48-h-treated groups ($P < 0.01$); however, there was no statistically difference between the 24-h- and 48-h-treated groups ($P > 0.05$). These results revealed that cell apoptosis was significantly induced by nonlethal dose of LPS/D-GalN challenge.

Expression of inflammatory cytokines in rat liver tissues following the LPS/D-GalN challenge

Acute liver injury induced by the simultaneous administration of LPS and D-GalN was closely associated with the production of inflammatory cytokines, such as TNF- α and IL-1 β [1, 2], especially TNF- α [20]. An earlier study had found that TNF- α and IL-1 β increase early in the circulation [6], leading us to ask whether the levels of these mediators also increase in the liver tissues of our experimental system. We therefore investigated the expression of TNF- α and IL-1 β genes in the liver tissues from the control and treated rats. As shown in Fig. 5A, the relative expression levels of TNF- α in control, 6-h-, 24-h- and 48-h-treated rats were 0.291 ± 0.037 , 0.305 ± 0.083 , 0.319 ± 0.116 and 0.274 ± 0.059 , respectively, indicating

that there were no statistically significant difference between the four group animals ($P > 0.05$). As shown in Fig. 5B, the relative expression levels of IL-1 β in control, 6-h-, 24-h- and 48-h-treated rats were 0.143 ± 0.074 , 0.701 ± 0.161 , 0.485 ± 0.109 and 0.507 ± 0.063 , respectively. The levels of IL-1 β levels in the control rats were significantly lower than those in the treated rats ($P < 0.01$). In addition, IL-1 β levels in the 6-h-treated rats were higher than those in the 24-h- and 48-h-treated rats, and no difference was found between the 24-h- and 48-h-treated rats.

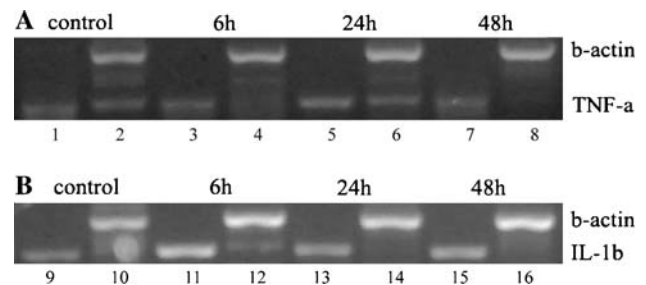
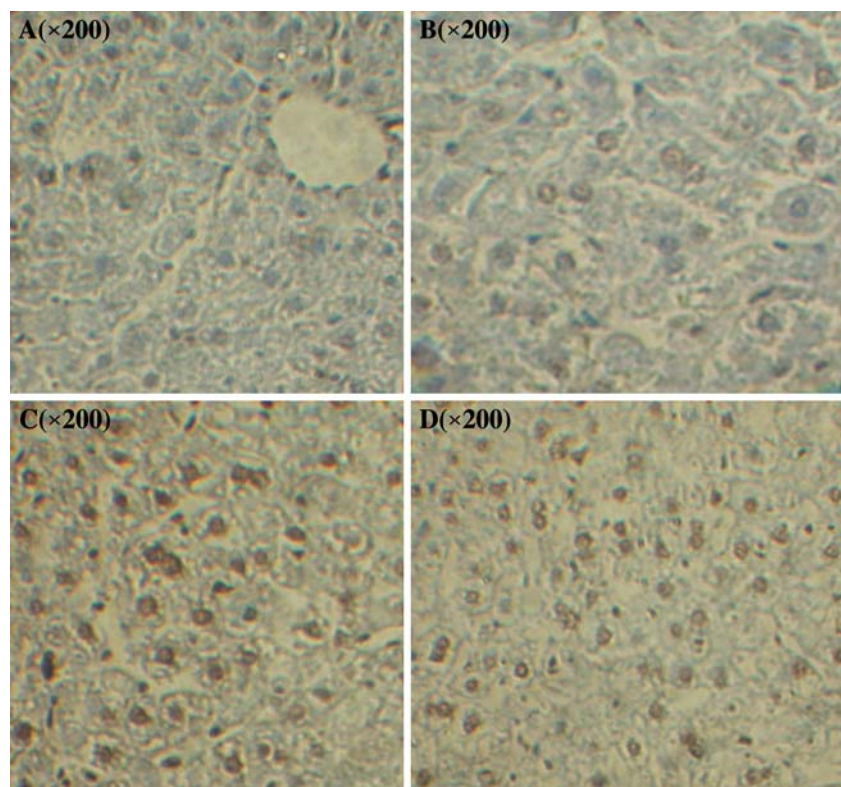


Fig. 5 Detection of tumor necrosis factor alpha (TNF- α) and interleukin 1 β (IL-1 β) mRNA in liver tissues of rats. mRNA expression of target genes or β -actin in the liver tissues of control rats and 6-h-, 24-h-, 48-h-treated rats. Lanes 1, 3, 5, 7, 9, 11, 13, 15 Target genes, lanes 2, 4, 6, 8, 10, 12, 14, 16 β -actin. Lengths of amplification products of TNF- α , IL-1 β and β -actin were 249, 372 and 621 bp, respectively

Fig. 4 The terminal transferase dUTP nick end labeling (TUNEL) assay of liver apoptosis from control and treated rats. **A** Control, **B** 6-h-treated group, **C** 24-h-treated group, **D** 48-h-treated group



Nitric oxide synthase mRNA was early induced by LPS/D-GalN in rat livers

An earlier study showed that NOS plays a critical part in immune-mediated liver injury [21] based on the observation that hepatic cytotoxicity usually correlated with the level of NO produced by iNOS. As shown in Fig. 6, the relative expression levels of iNOS in control, 6-h-, 24-h- and 48-h-treated rats were 0, 0.53 ± 0.16 , 0.36 ± 0.11 and 0.15 ± 0.04 , respectively. Significant differences were found among the three treated groups ($P < 0.01$). The results suggest that mRNA expression of iNOS was markedly induced by LPS/D-GalN, reaching a peak in the early period post-injection (6 h) and then gradually decreasing in a stepwise manner.

Expression of p53 mRNA in the livers of control and treated rats

p53, a tumor suppressor gene, plays a pivotal role in regulating cell apoptosis. It has been demonstrated that the elevated expression of p53 can lead to mitochondrial- or death receptor-mediated apoptosis [22]. As shown in Fig. 7, the relative expression levels of p53 in control, 6-h-, 24-h- and 48-h-treated rats were 0.031 ± 0.006 , 0.022 ± 0.010 , 0.49 ± 0.11 and 0.42 ± 0.17 , respectively. Statistically, the expression levels of the p53 gene in 24-h- and 48-h-treated rats were significantly higher than those in the control and 6-h-treated rats ($P < 0.01$), but no difference was found between the control and 6 h-treated rats ($P > 0.05$) or between the 24-h- and 48-h-treated rats ($P > 0.05$). These results suggest that overexpression of the p53 gene emerged

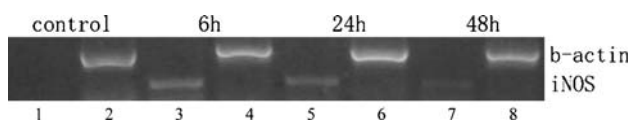


Fig. 6 Detection of inducible nitric oxide synthase (iNOS) mRNA in liver tissues of rats. mRNA expression of target genes or β -actin in the liver tissues of control and 6-h-, 24-h- and 48-h-treated rats. Lanes 1, 3, 5 and 7 target genes, lanes 2, 4, 6 and 8 β -actin. The length of the amplification products of iNOS and β -actin were 301 and 621 bp, respectively

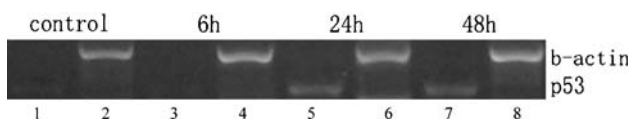


Fig. 7 Detection of TNF- α , IL-1 β , iNOS and p53 mRNA in liver tissues of rats. mRNA expression of target genes or β -actin in the liver tissues of control and 6-h-, 24-h- and 48-h-treated rats. Lanes 1, 3, 5, 7 target genes, lanes 2, 4, 6, 8 β -actin. The length of the amplification products of p53 and β -actin were 324 and 621 bp, respectively

in the crest-time of liver apoptosis (24 h) and maintained a high level until the late stage (48 h).

Activation of initiator and effector caspases in 24-h-treated rats

Intracellular aspartate-specific cysteine proteases (caspases) are the central mediators of apoptosis in mammalian cells. Initiator caspases, including caspase-8, -9 and -12 are closely associated with proapoptotic signals. Once activated, these caspases cleave and activate downstream effector caspases, such as caspase-3, which in turn execute apoptosis by cleaving cellular proteins following specific aspartate residues. We investigated the activation of these proteases in the crest-time of liver injury, which provided some cues on the different apoptotic signal pathways involved. As shown in Fig. 8, the activities of caspase-3, -8, -9, and -12 in 24-h-treated rat livers were 764.6 ± 137.8 , 70.3 ± 19.3 , 234.9 ± 31.7 and 138.5 ± 46.6 pmol/min.mg, respectively, whereas those in the control were 209.7 ± 49.4 , 9.2 ± 3.5 , 70.3 ± 10.6 and 17.7 ± 9.7 pmol/min.mg, respectively. The activities of caspase-3, -8, -9 and -12 in 24-h-treated rats were significantly higher than those in the control rats ($P < 0.01$). Therefore, we conclude that caspase-3, -8, -9, and -12 were activated by LPS/D-GalN challenge.

Discussion

LPS/D-GalN-induced hepatitis is a well-established model of liver injury. However, an earlier study showed that a combination of LPS and D-GalN resulted in the early death of major animals within 6–12 h [6]. The steep mortality of animals is a disadvantage to any mechanism research of

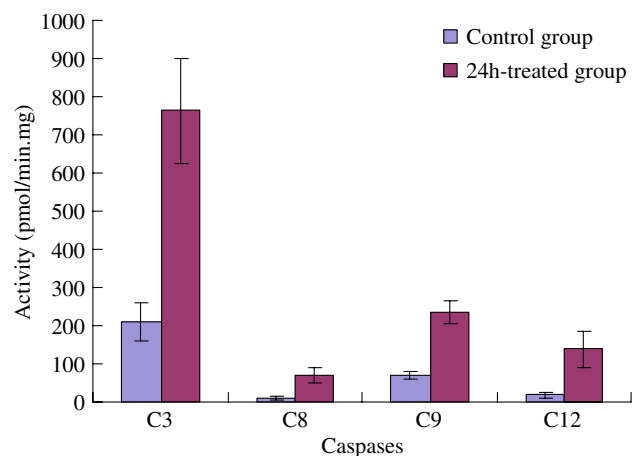


Fig. 8 Caspase activities in 24-h-treated or control rats. C3 Caspase-3, C8 caspase-8, C9 caspase-9, C12 caspase-12

hepatic injury and remote effect observation of drug treatment. An ideal animal model of liver injury should closely resemble ordinary liver injury in humans, with a longer clinical course and lower mortality. Therefore, in this study, we examined the disease course of liver injury induced by a nonlethal dose of LPS/D-GalN. We found that the characteristic indicators of acute liver injury or acute liver failure, such as abnormal blood biochemistry, inflammatory infiltration, erythrocyte agglutination and liver apoptosis or necrosis, appeared 6 h after LPS/D-GalN challenge and reached a peak at 24 h. At 48 h, although serum ALT began to degrade, widespread liver apoptosis and the destruction of liver architecture were still clearly evident based on histological observations and the TUNEL assay.

It is well-known that acute liver failure arises from an imbalance between hepatocellular death and regeneration [23]. There are two forms of hepatocellular death in acute liver failure: apoptosis and necrosis [24], with apoptosis considered to be the main pathological morphology. In addition, liver apoptosis has been demonstrated to play a pivotal role in virus- or nonvirus-induced acute liver injury [25–27]. As a general feature, the apoptosis of hepatocytes is the most important event in the molecular mechanisms of liver failure [28, 29] because apoptosis is the first cellular response of the liver to a wide range of toxic substances (including endotoxin) [27], and necrotic changes in hepatic tissues are often found to follow the appearance of apoptosis [30]. Hepatocellular apoptotic processes have been shown to play a significant role in the later development of necrosis in the liver [30]. Thus, an exploration of apoptotic or damaged mechanisms should provide an insight into the nature of endotoxin-induced acute liver injury.

It is clear that LPS does not directly induce the pathogenic roles, but rather the effects are caused indirectly via the action of inflammatory cytokines, such as TNF- α and IL-1 β (especially TNF- α). In other words, liver apoptosis or injury is mediated mainly by TNF- α [31, 32]. A previous study demonstrated that TNF- α levels rise very rapidly in the circulation, reaching a peak in plasma at 1 h [6]. Following the rise in TNF- α level, other cytokines, such as IL-1 β , also show a progressive rise in systemic levels [6]. However, it is unknown whether the high levels of these mediators exist in circulation or in the liver tissues at the stage of liver apoptosis. In the liver tissues examined here, IL-1 β mRNA levels appeared to peak at 6 h post-injection and remained at high levels at 24 and 48 h; however, no difference was found between the control and treated rats in terms of TNF- α mRNA expression levels. These results suggest that the maintenance of the inflammatory response of liver tissues could depend on the production of other inflammatory cytokines, such as IL-1 β and IL-6, followed by TNF- α ; in contrast, liver apoptotic death induced by

TNF- α must have had the participation of downstream damage or apoptotic genes.

Nitric oxide (NO) has been shown to play an important part in the survival or death of liver cells and to exhibit paradoxical functions, cytotoxicity and cytoprotection [33, 34]. The development of this double-edged role is dependent on the production of different NO synthases. Cytotoxicity is usually correlated with NO produced by iNOS. Our study showed that iNOS mRNA was induced by the LPS/D-GalN injection and that its level reached a peak in the early stage post-injection (6 h). Previous studies have found that an early burst in the TNF- α level could induce iNOS expression and result in apoptosis and necrosis of different types of cells through cytotoxic NO [35, 36]. We also examined the expression of the p53 gene. As the most important apoptosis-inducing gene in organisms, p53 plays a central role in inducing cell apoptosis. We found that the elevated expression of p53 runs parallel with massive liver apoptosis in the mid (24 h) and late (48 h) stages of this disorder, which implies an indispensable role of p53 in massive liver apoptosis induced by LPS/D-GalN challenge. There are at least three distinct but interactive apoptotic pathways in mammals: mitochondrial-mediated, death receptor-initiated and endoplasmic reticulum stress-mediated pathways [37, 38]. In response to cellular stress, p53 can stimulate a wide network of signals that act through at least two apoptotic pathways, the extrinsic, death receptor pathway and the intrinsic, mitochondrial one [22].

Following activation of these apoptotic signal cascades, the caspase family of cysteine proteases were activated. The initiator caspases can be activated by their respective apoptotic pathways; for example, caspase-8 is activated by the death receptor pathway, caspase-9 by the intracellular mitochondria pathway and caspase-12 by endoplasmic reticulum (ER) stress conditions. We found that caspase-3, -8, -9 and -12 were activated by LPS/D-GalN in 24 h-treated rats, thereby accounting for the activity of three important apoptosis pathways. The results may be of therapeutic implication of acute liver apoptosis or injury – that is to say, it may be difficult to reverse liver apoptosis through inhibiting only one or two of these pathways.

Acknowledgements We thank Jiang-jin Xu, Yu-chen Dai, Xiao-hua Qu, Jian-hong Jiang and Yai-qing Zou for valuable technical support. This study was supported by National Natural Scientific Grant of China (No.30660066, No.30360037)

References

1. Morrison DC, Danner RL, Dinarello CA et al (1994) Bacterial endotoxins and pathogenesis of Gram-negative infections: current status and future direction. *J Endotoxin Res* 1:71–83
2. Thirunavukkarasu C, Uemura T, Wang LF et al (2005) Normal rat hepatic stellate cells respond to endotoxin in LBP-independent

- manner to produce inhibitor(s) of DNA synthesis in hepatocytes. *J Cell Physiol* 204:654–665
3. Wang P, Chaudry IH (1996) Mechanism of hepatocellular dysfunction during hyperdynamic sepsis. *Am J Physiol Regulatory Integrative Comp Physiol* 270: R927–R938
 4. Bone RC, Balk RA, Cerra FB et al (1992) Definitions for sepsis and organ failure and guidelines for the use of innovative therapies in sepsis. The ACCP/SCCM consensus conference committee. American college of chest physicians/society of critical care medicine. *Chest* 101:1644–1655
 5. Galanos C, Freudenburg MA, Reutter W (1979) Galactosamine-induced sensitization to the lethal effect of endotoxin. *Proc Natl Acad Sci USA* 76:5939–5943
 6. Liu D, Li C, Chen Y et al (2004) Nuclear import of proinflammatory transcription factors is required for massive liver apoptosis induced by bacterial lipopolysaccharide. *J Biol Chem* 279(46):48343–48442
 7. Lehmann V, Freudenberg MA, Galanos C (1987) Lethal toxicity of lipopolysaccharide and tumor necrosis factor in normal and D-GalN-treated mice. *J Exp Med* 165:657–663
 8. Morikawa A, Kato Y, Sugiyama T et al (1999) Role of nitric oxide in lipopolysaccharide-induced hepatic injury in D-galactosamine-sensitized mice as an experimental endotoxin shock model. *Infect Immun* 67:1018–1024
 9. Dien MV, Takahashi K, Mu MM et al (2001) Protective effect of Wogonin on endotoxin-induced lethal shock in D-galactosamine-sensitized mice. *Microbiol Immunol* 45:751–756
 10. Thorlacius K, Slotta JE, Laschke MW et al (2006) Protective effect of fasudil, a Rho-kinase inhibitor, on chemokine expression, leukocyte recruitment, and hepatocellular apoptosis in septic liver injury. *J Leukoc Biol* 79:923–931
 11. Motobu M, Amer S, Koyama Y et al (2006) Protective effect of sugar cane extract on endotoxin shock in mice. *Phytother Res* 20(5):359–363
 12. Xiong Q, Hase K, Tezuka Y et al (1999) Acteoside inhibits apoptosis in D-galactosamine and lipopolysaccharide-induced liver injury. *Life Sci* 65:421–430
 13. Freudenberg MA, Keppler D, Galanos C (1986) Requirement for lipopolysaccharide-responsive macrophages in galactosamine-induced sensitization to endotoxin. *Infect Immun* 51:891–895
 14. Yin XM, Ding WX (2003) Death receptor activation-induced hepatocyte apoptosis and liver injury. *Curr Mol Med* 3:491–508
 15. Oreopoulos GD, Wu H, Szasz K et al (2004) Hypertonic preconditioning prevents hepatocellular injury following ischemia/reperfusion in mice: a role for interleukin 10. *Hepatology* 40:211–220
 16. McCarter SD, Akyea TG, Lu X et al (2004) Endogenous heme oxygenase induction is a critical mechanism attenuating apoptosis and restoring microvascular perfusion following limb ischemia/reperfusion. *Surgery* 136:67–75
 17. Ando K, Hiroishi K, Kaneko T et al (1997) Fas/Fas ligand and TNF- α pathways as specific and bystander killing mechanism of hepatic C virus-specific human CTL. *J Immunol* 158:5283–5291
 18. Yin M, Wheeler MD, Kono H et al (1999) Essential role of tumor necrosis factor alpha in alcohol-induced liver injury in mice. *Gastroenterology* 117:942–952
 19. Gantner F, Leist M, Lohse AW et al (1995) Concanavalin A-induced T-cell-mediated hepatic injury in mice: the role of tumor necrosis factor. *Hepatology* 21:190–198
 20. Kobayashi Y, Mori M, Naruto T et al (2004) Dynamic movement of cytochrome C from mitochondria into cytosol and peripheral circulation in massive hepatic cell injury. *Pediatr Int* 46:685–692
 21. Sass G, Koerber K, Bang R et al (2001) Inducible nitric oxide synthase is critical for immune-mediated liver injury in mice. *J Clin Invest* 107:439–447
 22. Haupt S, Berger M, Goldberg Z et al (2003) Apoptosis – the p53 network. *J Cell Sci* 116:4077–4085
 23. Thomson RK, Arthur MJ (1999) Mechanisms of liver cell damage and repair. *Eur J Gastroenterol Hepatol* 11:949–955
 24. Riordan SM, Williams R (2003) Mechanisms of hepatocyte injury, multiorgan failure, and prognostic criteria in acute liver failure. *Semin Liver Dis* 23:203–215
 25. Jaeschke H, Gujral JS, Bajt ML (2004) Apoptosis and necrosis in liver disease. *Liver Int* 24:85–99
 26. Kasahara I, Saitoh K, Nakamura K (2000) Apoptosis in acute hepatic failure: histopathological study of human liver tissue using the tunnel method and immunohistochemistry. *J Med Dent Sci* 47:167–175
 27. Doggrel SA (2004) Suramin: potential in acute liver failure. *Expert Opin Investig Drugs* 13:1361–1363
 28. Togo S, Kubota T, Matsuo K et al (2004) Mechanisms of liver failure after hepatectomy. *Nippon Geka Gakkai Zasshi* 105:658–663
 29. Eichhorst ST (2005) Modulation of apoptosis as a target for liver disease. *Expert Opin Ther Targets* 9:83–99
 30. Kobayashi M, Tsujitani S, Kurisu Y et al (2002) Bcl-2 and Bax expression for hepatocellular apoptosis in a murine endotoxin shock model. *Hepatogastroenterology* 49:1602–1606
 31. Leist M, Gantner F, Brohlinger I et al (1995) Tumor necrosis factor-induced hepatocyte apoptosis precedes liver failure in experimental murine shock models. *Am J Pathol* 146:1220–1234
 32. Morikawa A, Sugiyama T, Kato Y et al (1996) Apoptosis cell death in the response of D-galactosamine-sensitized mice to lipopolysaccharide as an experimental endotoxin shock model. *Infect Immun* 64:737–738
 33. Kim Y-M, Bergonia H, Lancaster JR (1995) Nitrogen oxide-induced autoprotection in isolated rat hepatocytes. *FEBS Lett* 374:228–232
 34. Kroncke K-D, Fehsel K, Kolb-Bachofen V (1997) Nitric oxide: cytotoxicity versus cytoprotection- how, why, when and where? *Nitric Oxide Biol Chem* 1:107–120
 35. Bonfoco E, Krainc D, Ankarcrona M et al (1995) Apoptosis and necrosis: two distinct events induced, respectively, by mild and intense insults with NMDA or nitric oxide/superoxide in cortical cell cultures. *Proc Natl Acad Sci USA* 92:7162–7166
 36. Lin K, Xue JY, Nomen M et al (1995) Peroxynitrite-induced apoptosis in HL-60 cells. *J Biol Chem* 270:16487–16490
 37. Ferri KF, Kroemer G (2001) Organelle-specific initiation of cell death pathways. *Nat Cell Biol* 3:E225–E263
 38. Scorrano L, Korsmeyer SJ (2003) Mechanisms of cytochrome C release by proapoptotic Bcl-2 family members. *Biochem Biophys Res Commun* 304:437–444